

ORIGINAL RESEARCH

Open Access

Pull-out behavior of galvanized steel strip in foam concrete

Maziar Ramezani*, Juan Vilches and Thomas Neitzert

Abstract

The interface and bond between concrete and reinforcing steel are the most fundamental problems of reinforced concrete structures. In this paper, the pull-out strength of galvanized steel strips with different geometries and hole patterns in foam concrete blocks are investigated experimentally and numerically. Foam concrete mixtures of 1,200-kg/m³ density were obtained by mixing cement and water in a mortar mixer together with ultrafoam as the foaming agent and Quick-Gel as the viscosifier. A theoretical model is developed to predict the bond-slip relationship between the strip and the concrete. This model is further implemented in a finite element simulation of the pull-out tests through the ABAQUS user subroutine. The results show good correlation between experimental, theoretical, and finite element simulation analyses. The influence of the steel strip geometries on the maximum pull-out force is also studied, and it was found that the strips with the greatest hole area, hole diameter, and circumference areas have higher pull-out forces and the increase is nearly linear.

Keywords: Bond stress-versus-slip relationship; Foam concrete; Pull-out test; Steel strip

Introduction

In the industrialized world, new and modern techniques and materials, such as composites, have become common in today's construction industry. These new materials are lightweight, energy efficient, aesthetically attractive, and efficiently handled and erected. Composite structural assemblies (CSAs) are products with performance superior to existing building elements, based on combinations of materials such as embedded light gauge steel components, settable fillers, and coatings of sheet materials to provide a variety of finishes (Akin et al. 2005). The materials are combined or assembled in various ways to provide improved performance in strength and stiffness and associated properties of acoustic filtering, thermal energy conservation, vibration resistance, moisture barriers or absorption, and fire behavior. The structural strength of these products is determined by the grade and thickness of the steel, the configuration of internal panel components, and by the features of infill material (Balendran et al. 2002).

The current paper focuses on novel materials for application in CSAs and the bonding performance between steel and infill materials. The bond between concrete and steel elements is one of the most important properties contributing to the successful functioning of a composite panel (Kayali 2004). The main contribution to bond strength comes from the chemical adhesion and the friction resistance occurring between the steel and the concrete as a result of the surface effects. Composite structures made of various materials can fail in several ways depending on material properties of components, design methods, and loading cases, but the most important is the cooperation of all elements (Alterman et al. 2011). The lack of compatibility between elements leads to bond failure, sliding of reinforcement bars and/or steel strips, local deformations, and finally cracking. Destructive measurements of shear strength through pull-out and push-in tests are commonly used methods to assess the quality of a connection between steel elements and fillers, e.g., concrete.

There are only few studies available in the literature about the structural bond properties between lightweight concrete and steel bars with pull-out test (see e.g., Cao and Chung 2001; De Lorenzis et al. 2002; Chang 2003; Al-mahmoud et al. 2007). Ben Romdhane and Ulm

* Correspondence: maziar.ramezani@aut.ac.nz
Centre for Advanced Manufacturing Technology (CAMTEC), School of Engineering, Auckland University of Technology, Auckland 1010 New Zealand

(2002) investigated the steel-concrete interface with computational mechanics. They modelled micro-to-macro mechanisms of the interface and studied the numerical implementation of this model in combination with a discrete crack model for concrete. Few finite element (FE) simulations of pull-out tests are also available in the literature (e.g., Wu et al. 2009; Wei et al. 2012), yet without accurate modelling of the interface and bond behavior. Casanova et al. (2012) presented a new finite element approach to model the steel-concrete bond effects. Their model proposed to relate steel, represented by truss elements, with the surrounding concrete in the case where the two meshes are not necessarily coincident. Most of the previous investigations about bonding behavior focused mainly on experimental and theoretical studies of shear stress between reinforcing bars and concrete specimens (e.g., Bouazaoui and Li, 2008; Fang et al. 2006; Khandaker and Hossain 2008), and plastic bars and concrete samples (e.g. Won et al. 2008), but not directly on steel strips, which are applicable to this project. This study investigates bonding performance and analyzes it through pull-out tests to provide data for the theoretical and FE analysis of CSAs. Because bonding is a general problem for wall panel design and other uses of concrete that employ steel to concrete contact zone, this research undertakes an analysis of the influence of various steel strip designs to understand bonding behavior. With the obtained results, the research enables understanding on the main features of metal face materials commonly used in wall panels.

Methods

Theoretical model

To have a better understanding of the pull-out test, a theoretical model is developed in this section which is suitable for pull-out test of a steel strip in concrete. The shear bond properties between the two materials can be determined by this model in the form of the bond stress-versus-slip relation. The model is based on the previous work of Banholzer et al. (2005), where the model is modified to fit the steel strip as the reinforcing element. Considering Figure 1, if an axial load P is applied at the end of the steel strip ($x = L$), the change in load dF_s over a distance dx along the strip is a function of the shear stress in terms of x and the circumference of the strip in contact with the concrete:

$$\frac{dF_s}{dx} = 2(a + b)\tau \quad (1)$$

where F_s is the force in the strip, a and b are the length and width of the steel strip cross section, and τ is the shear stress in the strip. By assuming that the interface is sheared due to an applied pull-out force and

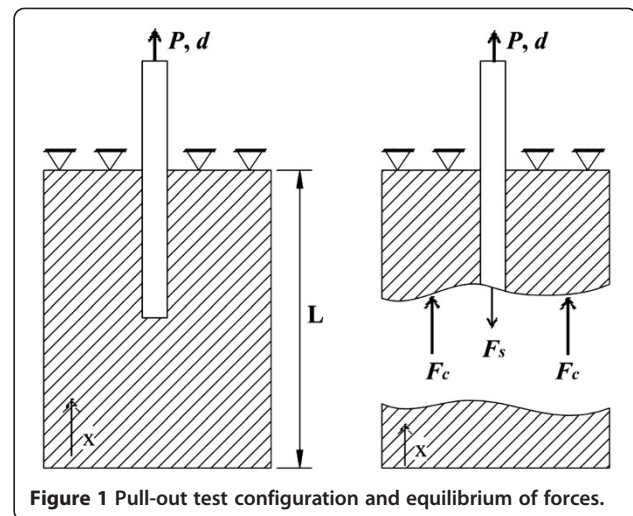


Figure 1 Pull-out test configuration and equilibrium of forces.

considering the absolute displacement of the concrete at a point x in relation to its origin as u_c and that of the strip as u_s , the slip s can be defined as the difference of u_c and u_s , as follows:

$$s = u_s - u_c. \quad (2)$$

Differentiating Equation 2 with respect to x yields

$$\frac{ds}{dx} = \varepsilon_s - \varepsilon_c \quad (3)$$

where ε_s and ε_c are the strain of the strip and the concrete, respectively. Using Hooke's law leads to

$$\frac{ds}{dx} = \frac{F_s}{E_s A_s} - \frac{F_c}{E_c A_c} \quad (4)$$

where E_s , A_s , E_c , and A_c are the modulus of elasticity of the strip in tension, the cross-sectional area of the strip, modulus of elasticity of the concrete in compression, and the load-carrying area of the concrete, respectively. As illustrated in Figure 1, the load application is idealized as a single pull-out load P at the top of the strip ($x = L$) with a corresponding displacement d applied in x direction. The global equilibrium of forces in an arbitrary chosen cross section yields

$$F_s + F_c = 0. \quad (5)$$

For demonstration purposes (see Figure 2), the relationship between τ and s is given as $\tau = \kappa s$, where κ is constant. It should be pointed out that a linear dependence between the shear stress and the slip is not

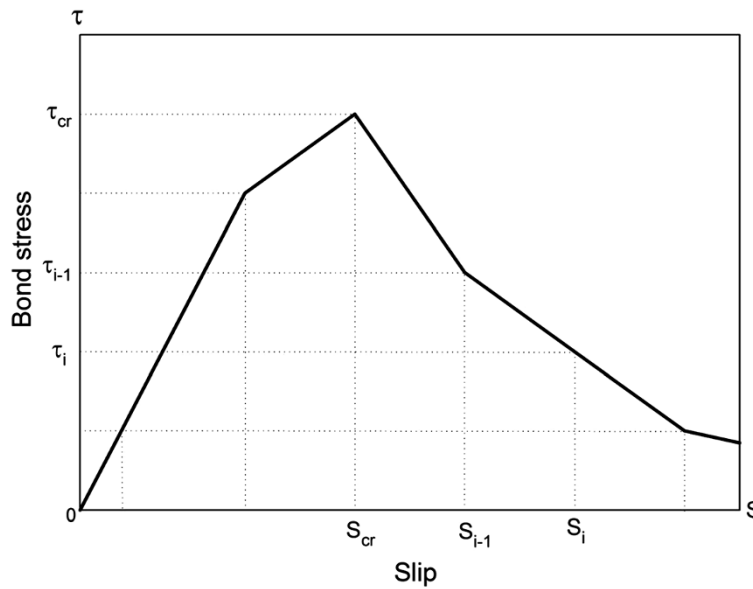


Figure 2 N piecewise linear relationship of bond stress versus slip.

assumed throughout the contact zone. The theoretical model uses a piecewise method where the nonlinear behavior of the contact interface is simplified by several linear pieces as illustrated in Figure 2. Combining these linear pieces gives a good approximation of the general nonlinear behavior. The pull-out problem can then be represented by a second-order differential equation, as follows:

$$F''_s - \beta^2 F_s = 0; \quad F_s(L) = P, \quad F_s(0) = 0$$

$$\beta^2 = 2(a + b) \left(\frac{1}{E_s A_s} + \frac{1}{E_c A_c} \right) \cdot k \quad (6)$$

where β is a material parameter which includes the bond stress-versus-slip relation. Another possible approach is to model the experimental situation in respect to the local slip s . After substituting Hooke's law for the strip and the

concrete respectively into Equation 3, differentiating the results with respect to x and using Equations 1 and 5, the following second-order differential equation in terms of s can be obtained:

$$s'' = 2(a + b) \left(\frac{1}{E_s A_s} + \frac{1}{E_c A_c} \right) \tau(s) = T(s)$$

$$T(s) = 2(a + b) \beta \tau(s) \quad (7)$$

$$\beta = \frac{1}{E_s A_s} + \frac{1}{E_c A_c}$$

$$s' = \beta F_s$$

Equation 7 represents the basic relationships between the second-order derivative of the local slip s and the local bond stress $\tau(s)$. Knowing that at $x = 0$ the force in the strip is zero ($s'(0) = 0$), assuming the slip s at the loaded strip end is d ($s(L) = d$), and denoting the

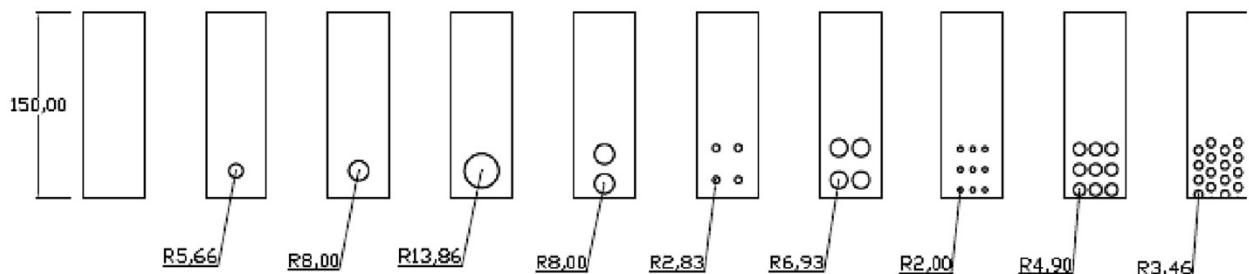


Figure 3 Patterns of holes in the steel strips (all sizes in mm).

coordinate of the strip by $0 \leq x \leq L$, the mathematical representation of the pull-out test can be expressed either as a boundary value problem

$$s'' = T(s), \quad s'(0) = 0, \quad s(L) = d \quad (8)$$

or as a corresponding initial value problem for a strip end slip δ at $x = 0$

$$s'' = T(s), \quad s'(0) = 0, \quad s(0) = \delta. \quad (9)$$

Banholzer et al. (2005) assumed an N piecewise linear bond law with no limitation of N (Figure 2) to achieve a general mathematical description of the bond law. The function $T(s) = 2(a + b)\beta\tau(s)$ can be expressed for an interval i ($s_{i-1} \leq s \leq s_i$) as

$$T(s) = m_i(s - s_{i-1}) + T_{i-1}, \quad (10)$$

$$m_i = \frac{T_i - T_{i-1}}{s_i - s_{i-1}}, \quad T_0 = s_0 = 0.$$

Consequently, the force F_s in the strip is normalized as well:

$$q(x) = \beta F_s(x) = s'(x). \quad (11)$$

The force in the strip at $x = L$ corresponds to the pull-out load P , and therefore, we have $s'(L) = q(L) = \beta P$. Now, the initial value problem (Equation 9) can be easily solved in an iterative process for any given $T(s)$ and δ , with Runge-Kutta numerical integration procedure, and the normalized pull-out force can be determined for a given displacement d , such that the boundary condition at the bottom of the strip $s'(0) = 0$ is satisfied.

Experimental analysis

Foam concrete mixtures were prepared at $1,200\text{-kg/m}^3$ density by using stable foam concrete compositions, which were designed based on the investigation of Kearsley and Mostert (2005). Properties of the foam concrete were

Table 1 Relationships of hole patterns

Hole pattern	Number of holes	Radius of holes (mm)	Area of holes (mm ²)
S0	0	0	0
S1-6	1	5.66	100.6
S4-3	4	2.83	100.6
S9-2	9	2	113.1
S1-8	1	8	201.1
S2-8	2	8	402.1
S14-3	14	3.46	526.5
S1-14	1	13.86	603.5
S4-7	4	6.93	603.5
S9-5	9	4.9	678.9



Figure 4 Testing mechanism with a freely adjustable ball joint and a plate with embedded bolts within foam concrete samples.

analyzed for density and compressive strength based on the standard testing methods for physical and mechanical properties (ASTM C495 and ASTM C39). Experiments showed that by using the theoretical design method of Kearsley and Mostert (2005), it is possible to predict the compressive strength and density for the concrete mixtures. Ordinary Portland Cement was used for the foam concrete mixtures. To prepare the foam, ultrafoam was used as the foaming agent and Quick-Gel (Baroid, Houston, TX, USA) as the viscosifier. These were mixed with water in the foam generator until the foam bubble size was uniform and stable (usually 2 min). Then, the foam was added to the cement matrix while stirring, with continual mixing for 1 to 2 min. When the mixture of foam and cement matrix was uniform, the prepared foam concrete was poured into the test mold with slight vibrations to fill up the mold completely. Specimens were demolded after 24 h and then moist cured in a standard curing room for a further 28 days in order to test the samples with a standard testing machine.

Standard cylinders of 100-mm diameter were used for the compressive strength tests, which were carried out in a testing machine of 100-kN capacity at a loading displacement rate of 0.1 mm/s. Three cylinders were tested for compressive strength after 28 days according to the ASTM C39 standard test method for compressive strength of cylindrical concrete specimens, and the mean value was

calculated. The average compressive strength of the foam concrete was 8.8 MPa.

The pull-out test method was used to evaluate the shear bonding strength between the steel and the foam concrete. All the pull-out tests followed the ASTM C900 standard. The ram velocity for all the tests was set at 0.2 mm/s to allow slow deformation of the concrete and the steel strips. The pull-out test samples include a foam concrete cube (100 mm × 100 mm × 100 mm) with galvanized steel sheet (50 mm × 150 mm) standing in the middle of the concrete cube. A hot-dip galvanized steel sheet, 0.75-mm thick, grade G250 from New Zealand Steel (Private Bag, New Zealand) was used. Steel sheets were pre-cleaned and degreased by using soapy water without damaging the coating before getting it in contact with the fresh concrete.

The influence of the steel strip geometries was studied as well. The major purpose of the pull-out test experiments was to investigate the effect of ten different hole patterns (Figure 3) in the steel strips on the bonding behavior. Ten different hole patterns were prepared including different numbers of holes (0, 1, 2, 4, 9, and 14), radius, and distribution (Table 1). The reason for using different sizes and numbers of holes was to investigate

the influence of contact cross section and hole patterns of the strip on the pull-out strength. These holes were filled with the concrete, and the effect of mechanical interlock produced by the concrete inside the holes will be studied. In codifying the hole pattern produced, steel plates were denominated as S0, S1-6, S4-3, S9-2, S1-8, S2-8, S14-3, S1-14, S4-7, and S9-5, for each number and approximate radius of holes.

Three specimens for each single set of strips were prepared and tested to determine the load-versus-displacement curves. Therefore, 30 tests had been carried out in total for all hole patterns. The primary pull-out tests showed that the results do not have significant variations, and therefore, it was decided to use three repetitions for each set of strip geometries. The pull-out tests were carried out using a universal testing machine equipped with a frame, which holds cubic samples and with a freely adjustable ball joint for pull-out tests as shown in Figure 4. Four M10 bolts were embedded through the cubic foam concrete samples and fixed to a plate at the bottom of the foam concrete cube to hold the sample in place. The adjustable ball joint for pull-out tests assures that the pull-out forces were centric to the strips during loading. The load was applied to the metal strip

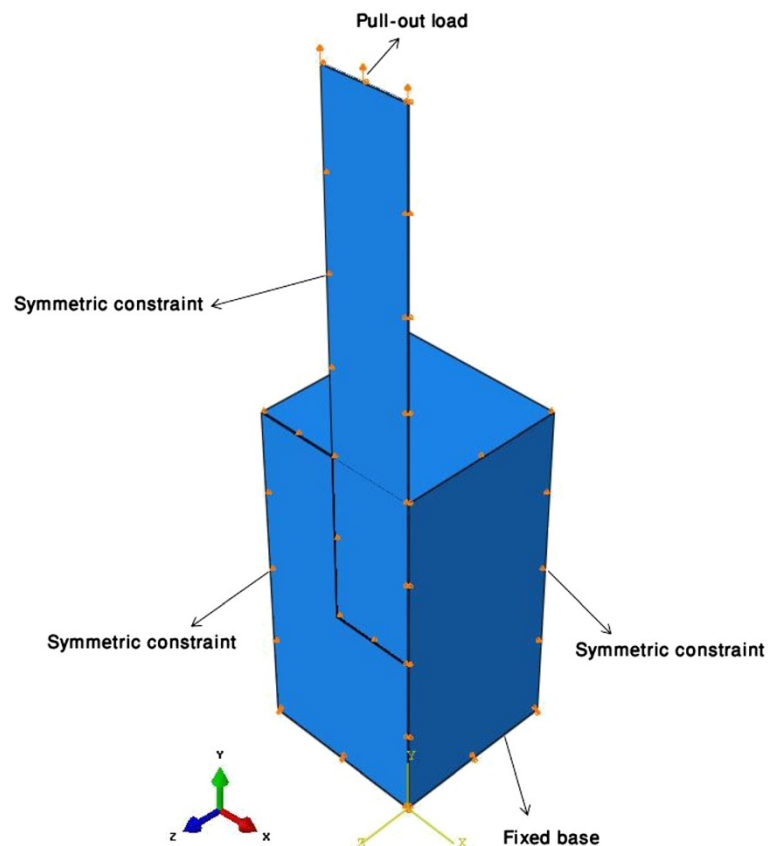


Figure 5 Load and boundary conditions for the FE model.

through a mechanical joint and evenly increased while controlling the displacement at a rate of 0.05 mm/s. Both the load applied and the displacement of the steel strip were measured and recorded on a computer until the strip was extracted from the cubic sample. Thus, a load-deformation curve was obtained from each experiment. It is worth pointing out that the slippage is not equal to the grip displacement throughout the contact zone. In the development of the theoretical model, it is only assumed that the slip s at the loaded strip end is equal to the grip displacement d ($s(L) = d$). The measured displacement is then related to the slip of the contact zone using the equations developed in the 'Theoretical model' section (see Equation 8).

Finite element simulations

The pull-out test was further studied by finite element simulations. A three-dimensional finite element model was developed using ABAQUS release 6.12 (Simulia, Providence, RI, USA) for this purpose. This is an implicit analysis code suitable for modelling both material and geometric nonlinearities and has good contact modeling. The FE analysis comprised an elastic-plastic simulation of the pull-out process and the determination of the load-displacement curve in the steel strip. The FE simulations were conducted for all the hole patterns depicted in Figure 3, and the FE results were compared with experimental and theoretical results. The material data for FE simulations were obtained from compression test of foam concrete and tensile test of steel strip. The galvanized steel sheet had the elastic modulus of 200 GPa and Poisson's ratio of 0.3 with the ultimate yield stress of 357 MPa. The foam concrete had a density of 1,200 kg/m³, Poisson's ratio of 0.2, and compressive strength of 8.8 MPa. The elastic modulus of the foam concrete was 5,535 MPa.

In the FE simulations, the bond stress-slip ($\tau - s$) relations obtained from experiments and theoretical modeling were used as the input data for the FE model. Bond stress-slip relations are considered as the constitutive relations for the behavior of the contact interface. The pull-out tests were then simulated by applying the shear constitutive behavior to the FE model by a user-defined subroutine. UINTER user-defined subroutine was used to define the interfacial constitutive behavior which proposes a new numerical model for simulating the bond-slip behavior of the composite structure. User subroutine UINTER is called at points on the slave surface of a contact pair with a user-defined constitutive model defining the interaction between the surfaces. The subroutine can be used to define the mechanical (normal and shear) interactions between surfaces. In this way, any special or proprietary interfacial constitutive behavior could be defined through the user subroutine UINTER written in FORTRAN in ABAQUS/Standard, which may include

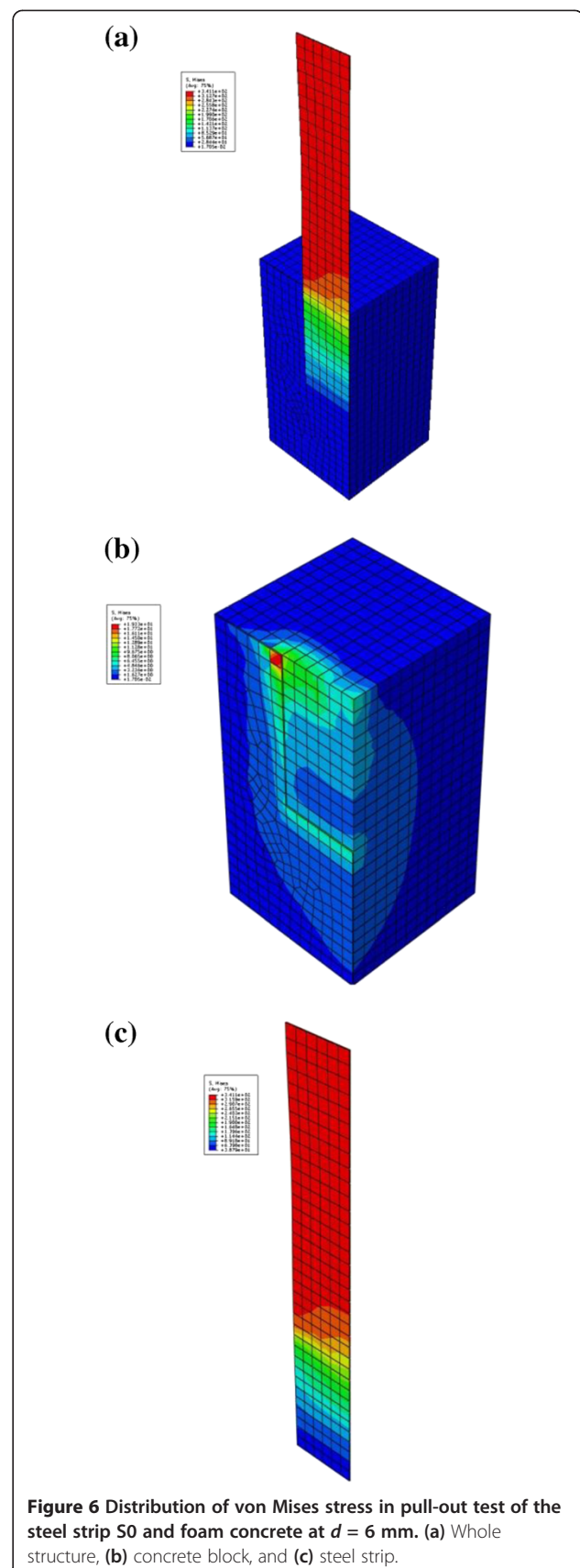


Figure 6 Distribution of von Mises stress in pull-out test of the steel strip S0 and foam concrete at $d = 6$ mm. (a) Whole structure, (b) concrete block, and (c) steel strip.

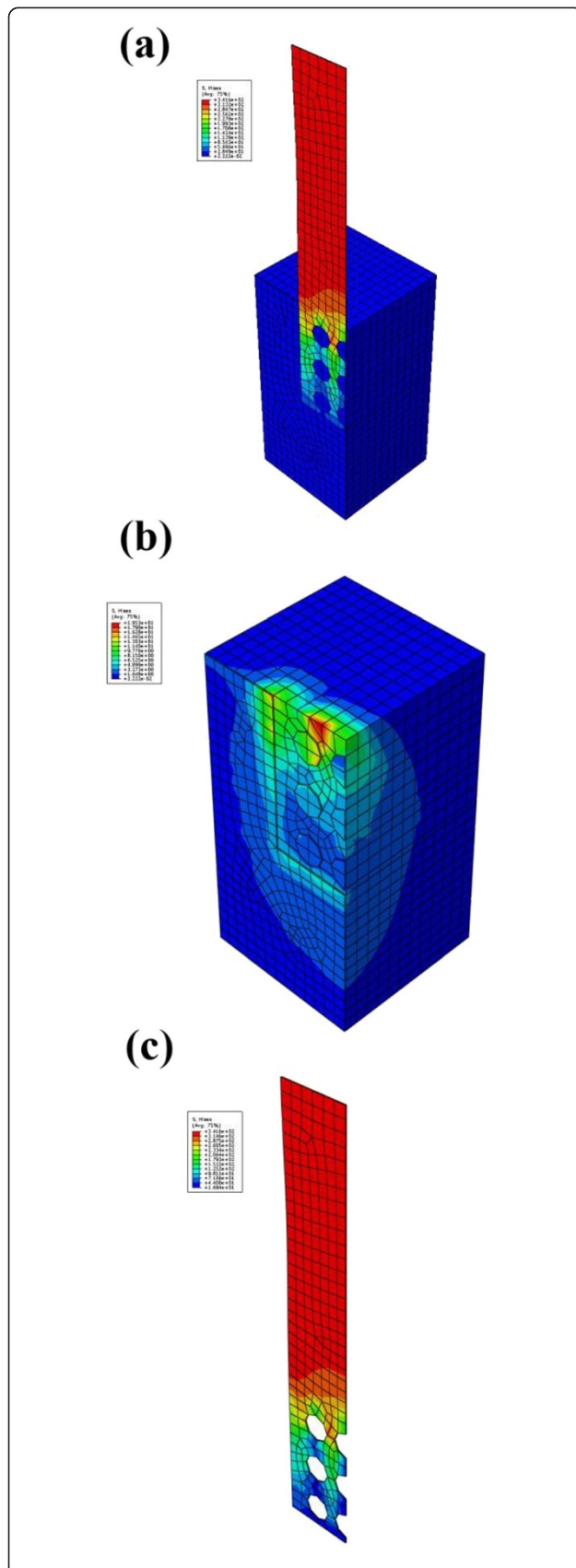


Figure 7 Distribution of von Mises stress in pull-out test of the steel strip S9-5 and foam concrete at $d = 6$ mm. (a) Whole structure, (b) concrete block, and (c) steel strip.

both the normal and tangential behaviors. This feature provides a strong tool for simulating the bond-slip behavior. User subroutine UINTER was called for each contact constraint location of affected contact pairs in every increment of the ABAQUS/Standard analysis. The input to this user subroutine includes the current relative position of a particular constraint point on the slave surface with respect to the corresponding closest point on the master surface, as well as the incremental relative motion between these two points. The normal direction constitutive behavior was modelled by using the penalty approach once the interaction surfaces are in contact; otherwise the normal strength is zero.

To minimize computation time, a quarter of the model was simulated due to symmetry and appropriate constraints were imposed on the symmetry plan. The load and boundary conditions are illustrated in Figure 5. The base of the concrete was fixed and the symmetry planes were constrained to model the actual behavior of the whole model. The pull-out load was applied to the top of the steel strip. The FE mesh was uniform and generated using C3D8R element which is an eight-node linear brick with reduced integration and hourglass control. Hourglass control formulation was used to control the distortion of solid elements during the final stages of the pull-out tests. The FE simulations were repeated without hourglass control, and the results clearly showed that the hourglass control formulation increases the accuracy of the model. In order to gauge how reasonable and accurate the results are on a given mesh, FE mesh convergence study was carried out. The results showed that the mesh size presented in Figure 6 produces a satisfactory balance of accuracy and computation time. The results showed that the finer mesh produced typically the same result; however, as the mesh was made finer, the computation time increased significantly.

The concrete damaged plasticity model was assumed for the concrete. The concrete damaged plasticity model provides a general capability for modelling concrete and other quasi-brittle materials in all types of structures. This model uses concepts of isotropic damaged elasticity in combination with isotropic tensile and compressive plasticity to represent the inelastic behavior of concrete. The concrete damaged plasticity model is based on the assumption of scalar (isotropic) damage and is designed for applications in which the concrete is subjected to arbitrary loading conditions. The model takes into consideration the degradation of elastic stiffness induced by plastic straining both in tension and

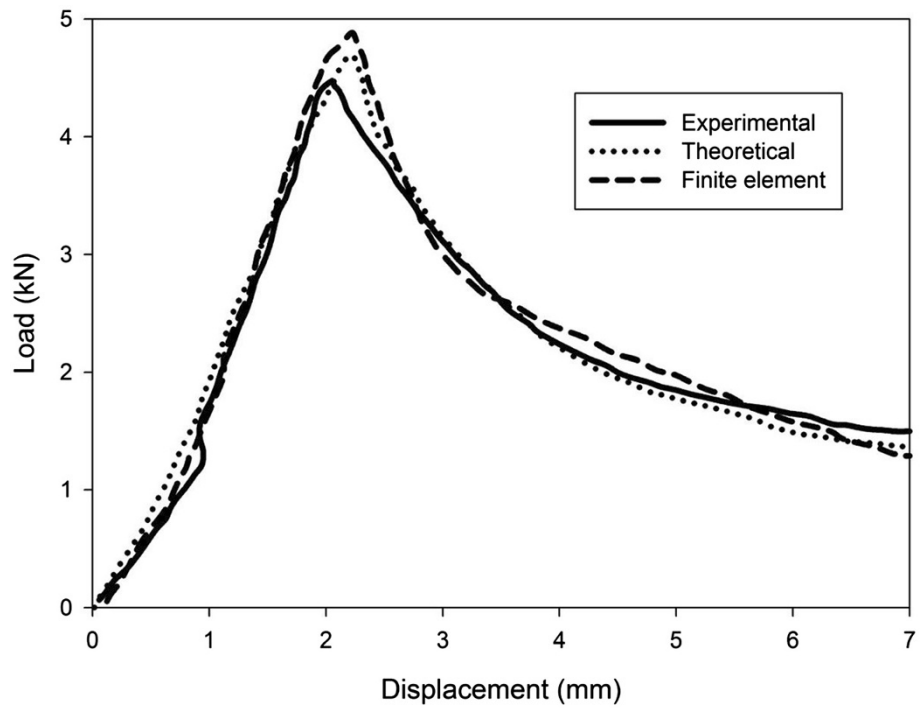


Figure 8 Load-displacement curves for the pull-out test of the steel strip S0.

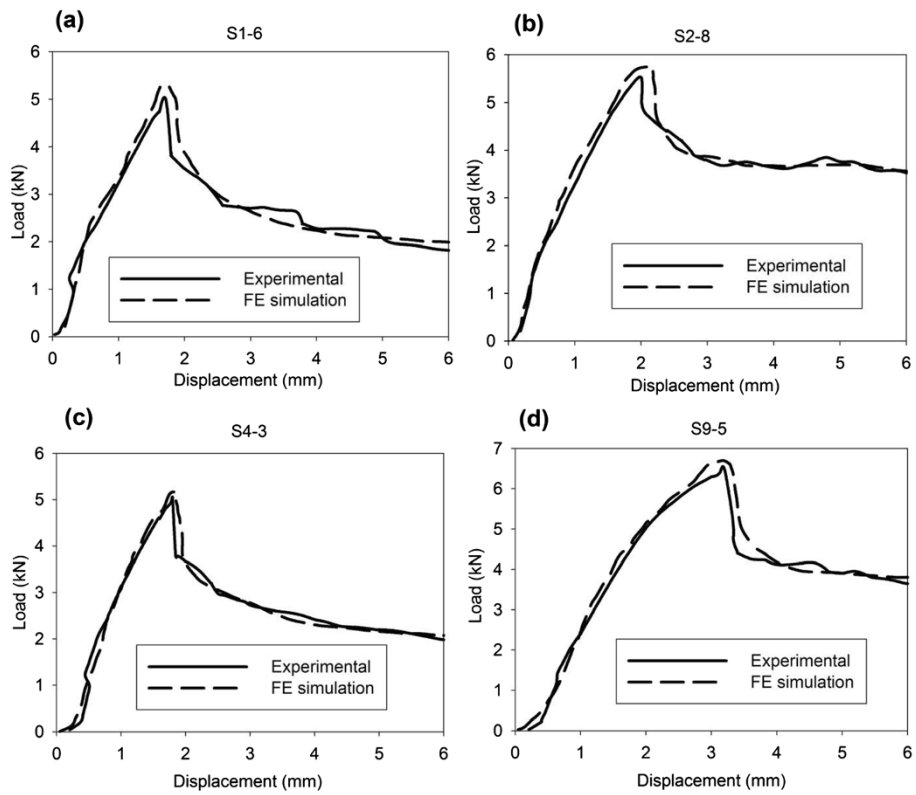


Figure 9 Load-displacement curves for the pull-out tests of the steel strips. (a) S1-6, (b) S2-8, (c) S4-3, and (d) S9-5.

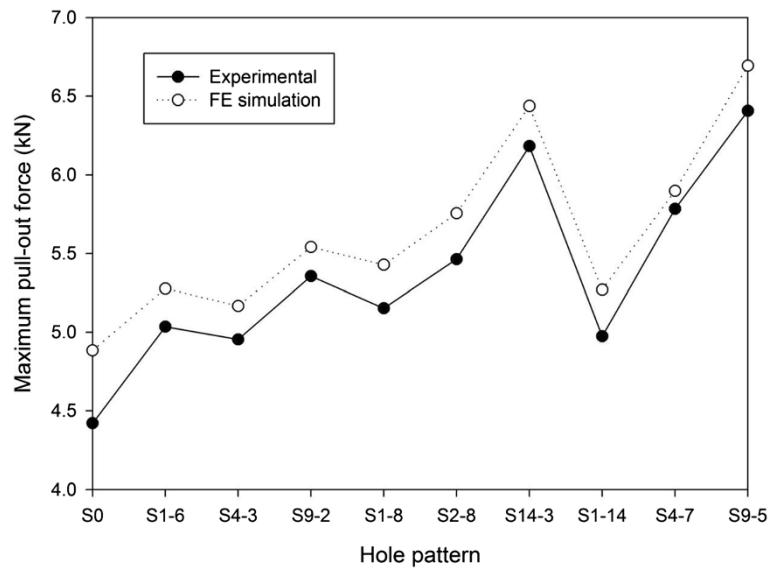


Figure 10 Comparison of experimental and FE simulation pull-out forces for different strip geometries.

compression. It also accounts for stiffness recovery effects under cyclic loading.

The node-to-surface contact between the strip and the concrete was modelled through the master-slave algorithm. General contact automatically assigns master and slave roles for contact interactions, and ABAQUS calculates an overclosure tolerance based on the size of the underlying element facets on a slave surface. Slave surfaces (or nodes) in a particular interaction are repositioned onto the associated master surface (or nodes) if the two surfaces are initially overclosed by a distance smaller than the calculated tolerance. Initial gaps between surfaces

remain unchanged by default adjustments. If a portion of a slave surface is initially overclosed by a distance greater than the calculated tolerance, ABAQUS automatically generates a contact exclusion for this surface portion and its associated master surface. Therefore, general contact does not create interactions between surfaces (or portions of surfaces) that are severely overclosed in the initial configuration of the model, and these surfaces can freely penetrate each other throughout the analysis.

A cohesive behavior was introduced between the contact surfaces. Cohesive behavior was defined as part of the surface interaction properties that are assigned to a

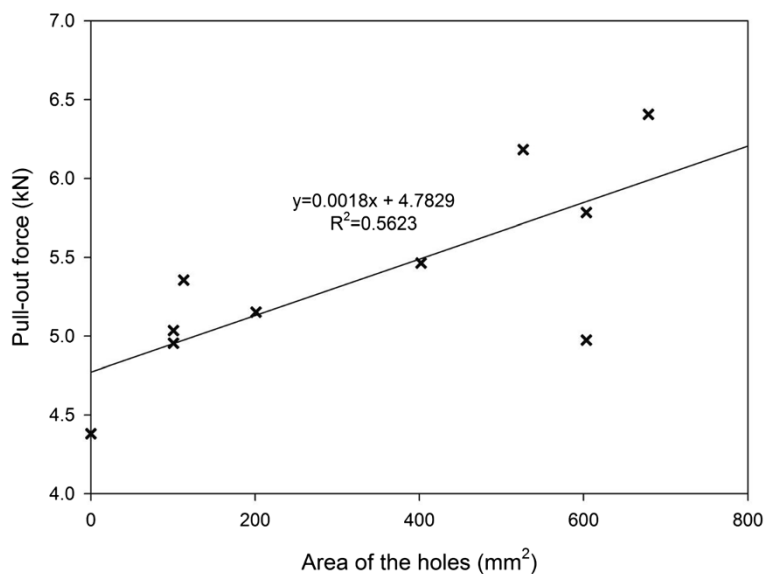


Figure 11 The effect of hole area on the pull-out force.

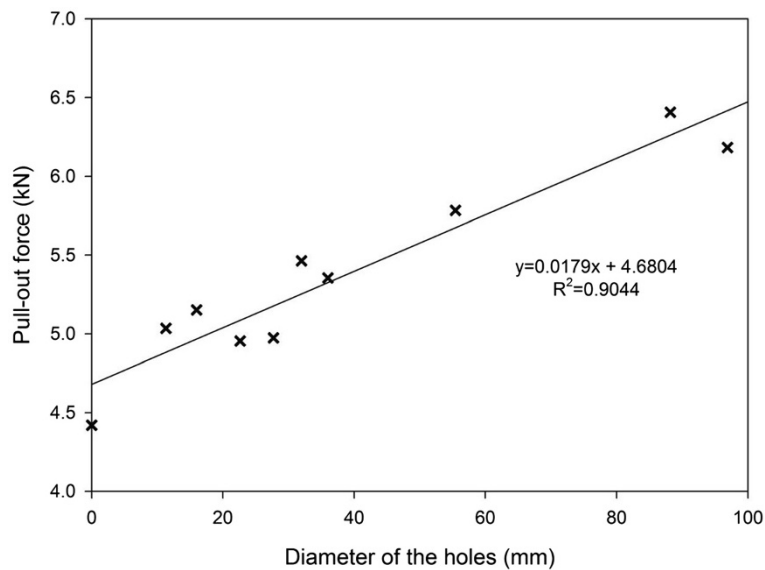


Figure 12 The effect of hole total diameter on the pull-out force.

contact pair. Surface-based cohesive behavior was defined as a surface interaction property and was used to model the surface interaction between the foam concrete and the strip. The cohesive behavior assumes that failure of the cohesive bond is characterized by progressive degradation of the cohesive stiffness, which is driven by a damage process. It also allows the failed nodes to re-enter contact with post-failure cohesive behavior. The nonlinear geometry NLGEOM option in ABAQUS was used throughout the analysis. Figures 6 and 7 show the distributions of the von Mises stress in the strips and

the concrete blocks in the pull-out tests of the steel strips S0 and S9-5, respectively.

Results and discussions

The results of the pull-out tests between the steel strips and the aerated concrete, and theoretical and FE analyses are presented and discussed here. The main purpose of the pull-out experiments was to find relationships between ten-hole patterns and mechanical properties of aerated concrete in order to evaluate and predict the bonding

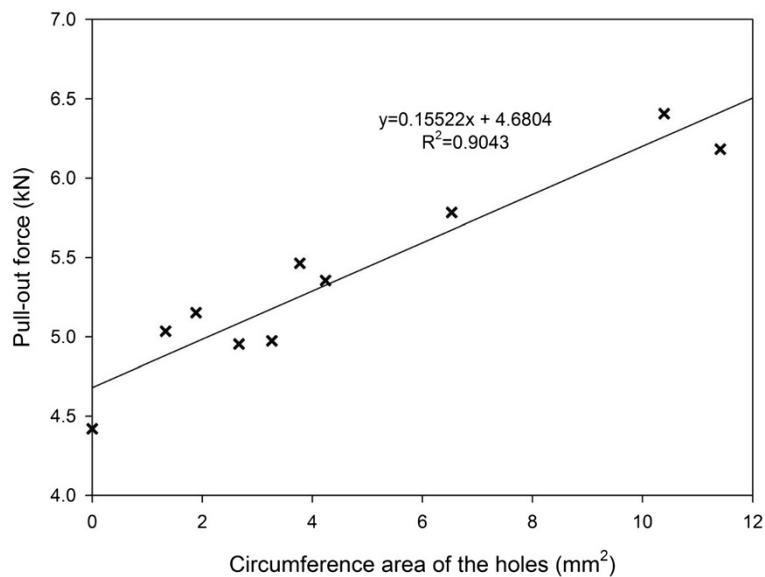


Figure 13 The effect of hole circumference area on the pull-out force.

between steel and lightweight concrete through a numerical simulation.

Three specimens for each single set (three identical samples) of strip design were prepared and tested to determine the bonding strength during pull-out tests. The reference hole area was 100.6 mm^2 with a 11.32-mm diameter. The reference area was increased gradually in order to verify the effect of the anchorage of the concrete embedded into holes in various designs.

The load-displacement curves for the original pull-out test of the steel strip without hole is depicted in Figure 8 for the experimental, theoretical, and FE simulation analyses. It can be seen from the figure that the results show very good correlation, with the FE model predicting slightly higher pull-out force. It is worth pointing out that the theoretical model developed in the section 'Theoretical model' is only valid for the pull-out test of the steel strip without any hole in terms of predicting the load-displacement curve. However, the bond-slip relationship obtained from this model can be further used in FE simulations of all other strip geometries through the user-defined subroutine UINTER. The load-displacement curves obtained from the experiments and FE simulations for all other strip geometries were also compared and show very good agreement. For brevity, only the results for four cases, S1-6, S2-8, S4-3, and S9-5, are presented in Figure 9; however, all other cases show the same trend. It can be seen from the figure that the pull-out load drops suddenly after the maximum value is achieved and then starts to decrease slowly, which indicates that the loading capacity still exists even after debonding. It is found from pull-out experiments that a long softening stage ($>20 d_1$) exists after the maximum load, where d_1 is the displacement corresponding to the maximum pull-out load. The experimentally and FE simulation predicted maximum pull-out forces were measured and depicted in Figure 10 for all the hole patterns. In general, the FE simulations tend to predict slightly higher pull-out force as shown in Figure 10 with the differences less than 10%.

Figures 11, 12 and 13 illustrate the maximum pull-out force for all pull-out results of the ten series of samples with respect to the total hole area, the total diameter of the holes, and the total circumference area of the holes, respectively. According to Figure 11, a correlation coefficient of $R^2 = 0.5623$ was achieved, which shows a weak relationship of data for different hole patterns. However, it can be seen that by discarding the S1-14 sample, the correlation improves greatly. Figures 12 and 13 show strong correlations of $R^2 = 0.9044$ and $R^2 = 0.9043$, respectively. In general, the figures reveal that there is a nearly linear increase of the pull-out forces on steel strips with holes with respect to specimens without holes if the hole sizes are similar. In general terms, pull-out force increases when all the three parameters (total

hole area, diameter, and circumference area) increase. The main reason for the different behavior of S1-14 is that the area of chemical adhesion was reduced due to the holes cut into the steel strips, and the mechanical interlock introduced by the concrete inside the holes is not enough to compensate for the loss of adhesion in weaker matrix.

Conclusions

The goal of this paper was to describe bonding processes between steel and concrete specimens experimentally and by applying analytical and FE methods. The results of investigations on the bonding behavior between lightweight concrete and steel strips enable a better understanding on the use of lightweight concrete in wall panels. The results show that the experimental, theoretical, and FE simulation results match very well. Three geometrical parameters affecting the pull-out force were also investigated in this paper, namely the total area of the holes, the diameter of the holes, and the circumference area of the holes. The diameter of the holes or circumference area of the holes was found to give stronger correlation with the pull-out forces; however, weaker correlations exist between the pull-out forces and the total area of the holes. The strips with the greatest hole area, hole diameter, and circumference areas had higher pull-out forces, and the increase is nearly linear.

Competing interests

The authors declare that they have no competing interests.

Authors' contributions

MR carried out the theoretical and finite element simulation analyses. JV conducted the experimental tests and assisted the simulations. TN participated in the study design and team supervision. All authors contributed to and approved the final manuscript.

Acknowledgements

The authors like to thank the Foundation of Research, Science and Technology (FRST) of New Zealand for the generous financial support received during the investigation.

Received: 23 June 2013 Accepted: 30 August 2013

Published: 27 September 2013

References

- Akin O, Gül R, Cüneyt A (2005) Effect of steel fibers on the mechanical properties of natural lightweight aggregate concrete. *Mater Lett* 59:3357–3363
- Al-mahmoud F, Castel A, François R, Tourneur C (2007) Effect of surface pre-conditioning on bond of carbon fibre reinforced polymer rods to concrete. *Cement Concrete Comp* 29:677–689
- Alterman D, Vilches J, Neitzert T (2011) An analysis of the bonding energy through pull-out tests for aerated concrete with various steel strip geometries. *Adv Mater Res* 275:55–58
- Balendran RV, Zhou F, Nadeem A, Leung A (2002) Influence of steel fibres on strength and ductility of normal and lightweight high strength concrete. *Build Environ* 37:1361–1367
- Banholzer B, Brameshuber W, Jung W (2005) Analytical simulation of pull-out tests—the direct problem. *Cement Concrete Comp* 27:93–101
- Ben Romdhane MR, Ulm FJ (2002) Computational mechanics of the steel-concrete interface. *Int J Numerical Anal Methods Geomechanics* 26(2):99–120
- Bouazaoui L, Li A (2008) Analysis of steel/concrete interfacial shear stress by means of pull out test. *Int J Adh & Adhes* 28:101–108

- Cao J, Chung D (2001) Degradation of the bond between concrete and steel under cyclic shear loading, monitored by contact electrical resistance measurement. *Cem Concr Res* 31:669–671
- Casanova A, Jason L, Davenne L (2012) Bond slip model for the simulation of reinforced concrete structures. *Eng Struct* 39:66–78
- Chang J (2003) Bond degradation due to the desalination process. *Construct Build Mater* 17:281–287
- De Lorenzis L, Rizzo A, La Tegola A (2002) A modified pull-out test for bond of near-surface mounted FRP rods in concrete. *Composites: Part B* 33:589–603
- Fang C, Lundgren K, Plos M, Gylltoft K (2006) Bond behaviour of corroded reinforcing steel bars in concrete. *Cem Concr Res* 36:1931–1938
- Kayali O (2004) Bond of steel in concrete and the effect of galvanizing. *Galv Steel Reinf Concr* 8:229–270
- Kearsley EP, Mostert HF (2005) Designing mix composition of foam concrete with high fly ash contents. *Use of foamed concrete in construction*. ICE, London, In, pp 29–36
- Khandaker M, Hossain A (2008) Bond characteristics of plain and deformed bars in lightweight pumice concrete. *Construct Build Mater* 22:1491–1499
- Wei G, Liu G, Xu C, Sun X (2012) Finite element simulation of perfect bonding for single fiber pull-out test. *Adv Mater Res* 418–420:509–512
- Won J, Park C, Kim H, Lee S, Jang C (2008) Effect of fibers on the bonds between FRP reinforcing bars and high-strength concrete. *Composites: Part B* 39:747–755
- Wu JJ, Cheng XH, Qi Y (2009) Simulation and analysis of single fibre pull-out test with FEM. *Shanghai Jiaotong Daxue Xuebao/Journal of Shanghai Jiaotong University* 43(10):1601–1604. 1608

doi:10.1186/2008-6695-5-24

Cite this article as: Ramezani et al.: Pull-out behavior of galvanized steel strip in foam concrete. *International Journal of Advanced Structural Engineering* 2013 5:24.

Submit your manuscript to a SpringerOpen[®] journal and benefit from:

- ▶ Convenient online submission
- ▶ Rigorous peer review
- ▶ Immediate publication on acceptance
- ▶ Open access: articles freely available online
- ▶ High visibility within the field
- ▶ Retaining the copyright to your article

Submit your next manuscript at ▶ springeropen.com
